Hindawi Publishing Corporation
Advances in Materials Science and Engineering
Volume 2013, Article ID 408347, 7 pages
http://dx.doi.org/10.1155/2013/408347

Research Article

Misfit in Inconel-Type Superalloy

Pavel Strunz,[1] Martin Petrenec,[2,3] Vadim Davydov,[4] Jaroslav Polák,[2,5] and Přemysl Beran[1]

[1] *Nuclear Physics Institute, ASCR, 25068 Řež, Czech Republic*
[2] *Institute of Physics of Materials, ASCR, Žižkova 22, 61662 Brno, Czech Republic*
[3] *TESCAN ORSAY HOLDING, a.s., Libušina tř. 21, 62300 Brno, Czech Republic*
[4] *Materials Science and Simulation, ASQ/NUM, PSI, 5232 Villigen, Switzerland*
[5] *CEITEC IPM, Institute of Physics of Materials, ASCR, 61662 Brno, Czech Republic*

Correspondence should be addressed to Pavel Strunz; strunz@ujf.cas.cz

Received 22 August 2013; Revised 21 November 2013; Accepted 27 November 2013

Academic Editor: Debashis Mukherji

An important parameter for the characterization of microstructural changes in nickel base superalloys is the misfit - the relative difference between lattice parameters of γ matrix and γ' precipitates. The misfit in IN738LC superalloy was examined at POLDI time-of-flight (TOF) neutron diffractometer both at room temperature and in situ at elevated temperatures using a high-temperature furnace. A careful out-of-furnace measurement yielded the lattice parameters of both γ and γ' phase at room temperature (a_γ = 3.58611(10) Å, $a_{\gamma'}$ = 3.58857(17) Å) as well as the misfit (equal to $6.9(6) \times 10^{-4}$). The in situ measurement at elevated temperatures provided the temperature dependence of the lattice parameters of γ (up to 1120°C) and γ' (up to 1000°C). Using these data, the evolution of the misfit with temperature was calculated. The misfit decreases with increasing temperature until it reaches zero value at a temperature around 800°C. Above 800°C, it becomes negative.

1. Introduction

The excellent strength of Ni-base superalloys [1] comes from their microstructure composed of strengthening cuboidal γ'-precipitates with an ordered structure $L1_2$ coherently embedded in γ solid solution phase (fcc) [2]. The critical parts of gas turbines made of superalloys are subjected to cyclic elastic-plastic straining as a result of heating and cooling during start-up and shut-down periods. Low-cycle fatigue damage and thus microstructural changes are induced in service. An important parameter for the characterization of the microstructure and the microstructural changes is the misfit of both phases. It is defined as the relative difference between the lattice parameters of γ' precipitates and γ matrix; that is, it is equal to $2(a_{\gamma'} - a_\gamma)/(a_{\gamma'} + a_\gamma)$. The misfit is related to coherency stresses and thus to the γ/γ' interfacial energy. Influence of misfit on γ'-precipitates coarsening is thus expected [3]. Superalloys with small misfit perform better in this regard. Also, creep resistance can be affected by misfit magnitude and sign as the misfit stresses influence dislocation activity in γ channels [4]. More important is the misfit at operational temperatures and, therefore, the misfit and its evolution with temperature are a subject of interest [4–8].

Neutron diffraction (ND) [9] offers a unique tool for ex- or in situ investigation of the misfit in the bulk of cast superalloys containing large grains. X-ray powder diffraction can be hardly used for the misfit determination in the Inconel alloy investigated in this study due to the millimeter-size grains and, therefore, their insufficient number in the gauge volume for X-ray scattering.

In order to supplement the results of other tests [2, 10, 11] by information on the misfit in superalloy IN738LC, the misfit was studied by means of ND at room temperature and also in-situ at elevated temperatures. Using in situ ND, the evolution of the misfit can be obtained directly at operational temperatures.

2. Experimental

2.1. Superalloy Samples. In the present experiment, the second-generation polycrystalline nickel base superalloy

Table 1: The composition of IN738LC superalloy [12].

Element	Cr	Mo	C	Co	Fe	Zr	Nb	Al	B	Ti	Ta	W	Ni
Content (wt%)	16.22	1.71	0.10	8.78	0.20	0.04	0.84	3.35	0.008	3.37	1.77	2.63	Balance

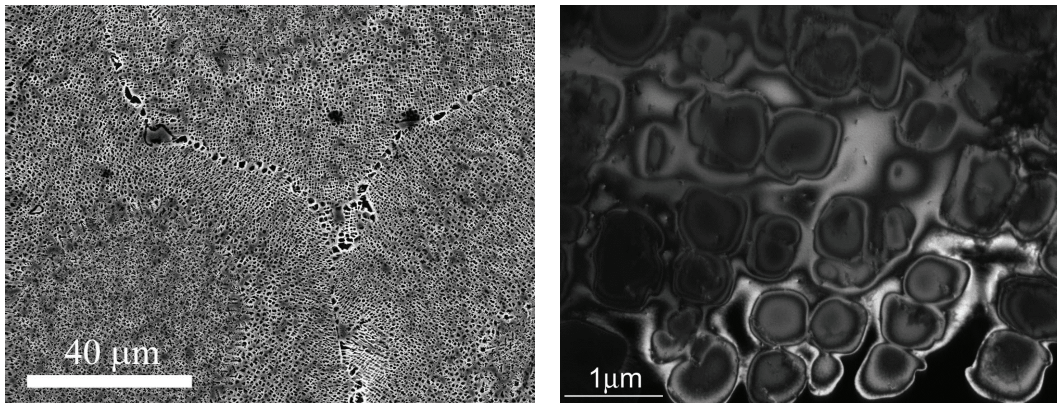

(a) (b)

Figure 1: Micrographs of the investigated IN738LC superalloy in as-delivered conditions: (a) SEM (secondary carbides at grain boundaries are visible as well) and (b) TEM.

IN738LC (LC stands for "low carbon") delivered by PBS Turbo Velká Bíteš a.s. (CZ) was used. The superalloy has an elevated percentage of Cr in order to enhance corrosion resistance. Its chemical composition is shown in Table 1.

The as-delivered material was already in heat-treated conditions (solution treatment at 1120°C for 2 hours, air cooling, and precipitation treatment at 845°C for 24 hours followed by air cooling). Figure 1 displays micrographs of the typical precipitate microstructure in the material. The morphology of γ' precipitates is mostly cuboidal with dimensions in the range 1000–7000 Å [13]. The precipitate volume fraction is around 50% [2, 14, 15]. For Inconel-type superalloys, the misfit is generally less than 0.5%.

The investigated specimens of IN738LC were identical cylindrical bars (denoted by A, B, and C in what follows) with diameter of 5 mm. The important characteristic of IN738LC is that it has very coarse grains, up to millimeter size.

2.2. Neutron Diffraction. The misfit in IN738LC alloy was examined using POLDI time-of-flight (TOF) neutron diffractometer at SINQ (PSI, Villigen, Switzerland) [16]. Before the experiment, the device was calibrated with α-Fe and Si powders.

The slit in front of the sample had a width of 3.8 mm and a height of 20 mm. The detector center was at an angle of $\Delta 2\theta = 89.5^\circ$ with respect to the primary beam (see scheme in Figure 2) and its angular extent was $\pm 15^\circ$. A radial collimator was placed between the sample and the detector. It selected 3.8 mm width of the scattered beam in the sample position (see Figure 2; the square $3.8 \times 3.8\ \text{mm}^2$ determining the top-view cut through the measured volume is displayed, too). Therefore, the gauge volume was estimated to be $3.8 \times 3.8 \times 20\ \text{mm}^3 = 290\ \text{mm}^3$. However, due to the extralarge grain size (≈1 mm) in IN738LC, the number of grains in the gauge volume was rather low.

The misfit in IN738LC alloy was examined out of furnace as well as in furnace (in situ) at elevated temperatures in high-temperature furnace.

2.2.1. Out-of-Furnace Measurements. The large grains in the alloy can cause artificial shifts of peak positions with respect to their expected places. It occurs due to the inhomogeneous distribution of the scattering power for a particular reflection (see Figure 2). This effect was confirmed in our samples by preliminary fits carried out after measurements with a stationary (i.e., not rotating) sample or with a sample rotating only in a limited (i.e. less than 360°) angular range. The peak shifts were evident in such a case. The position relations between the individual reflections could not be precisely fulfilled without introducing the peak shifts (different for different *hkl* reflections).

In order to simulate symmetrical distribution of the scattering power, the samples (denoted A and C) examined out of furnace were continuously ω-rotated by 360° during collection of the diffractograms. This procedure made the time-averaged scattering power of the sample symmetrical with respect to the axis of rotation for all the reflections and, therefore, no shifts of peaks with respect to their expected positions occurred (i.e. the position relations between the individual reflections were precisely fulfilled for the 360°-rotating sample). This out-of-furnace measurement with 360°-rotating sample was thus taken as a reference for the precise lattice parameter determination of both γ and γ' phases at RT ($a_{\gamma\text{RT}}$ and $a_{\gamma'\text{RT}}$).

An asymmetry in the peak shapes for nonrotating sample (or for a sample rotating less than 360°) could occur as well. This would happen, for example, if a large grain in one part

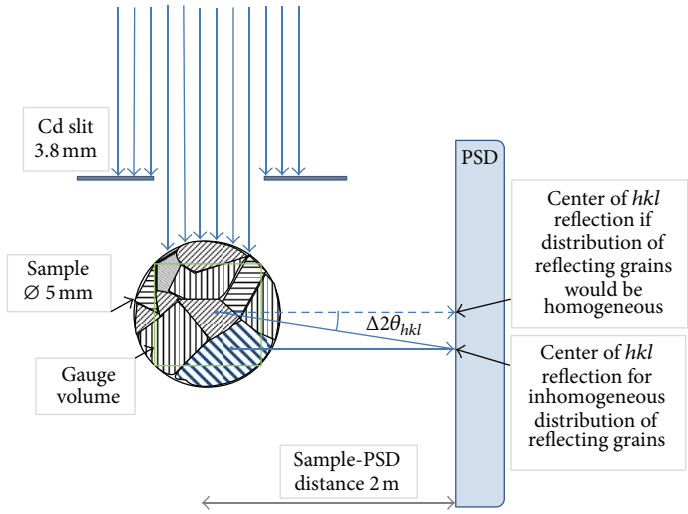

FIGURE 2: Scheme (top view) of the out-of-furnace measurement. If the sample is not ω-rotating in the range of 360° during the measurement, the reflection can be shifted by $\Delta 2\theta_{hkl}$ with respect to the expected position as it can originate from a large excentric grain. The $\Delta 2\theta_{hkl}$ shifts are different for different reflections as different grains scatter.

of the sample scatters to a particular reflection together with a smaller grain in the opposite part of the sample and both contribute to the same reflection. Nevertheless, no significant asymmetry was observed for the investigated samples. Most probably, large asymmetries did not happen due to the very large grains; that is, for every reflection only one grain scattered at once. It was apparent from two-dimensional data 2θ-TOF for measurement with nonrotating sample. Possible small asymmetries could not be resolved due to the limited resolution of POLDI diffractometer

2.2.2. In-Furnace Measurements at RT. During the in-furnace measurement (sample denoted B) at RT, it was not possible to rotate the sample (together with the sample environment) during the collection of the diffractogram more than 60° as the furnace geometry did not allow larger rotations.

Therefore, artificial peak shifts $\Delta 2\theta_{hkl}$ with respect to their expected positions $2\theta_{hkl}$ were again found, similarly as in case of the nonrotating out-of-furnace measurement (see Figure 2). The shifts $\Delta 2\theta_{hkl}$ varied randomly (both positive and negative values were recorded) for varying lattice planes *hkl*. This effect occurred most likely due to the abovementioned large grains, causing an eccentric distribution of the scattering power for any measurement with insufficiently rotating sample (see Figure 2). If this explanation holds, the observed shifts $\Delta 2\theta_{hkl}$ would be in the range $\pm 1 \times 10^{-3}$ rad (±0.05°), which corresponds to the gauge size (determined by the radial collimator) and sample-to-detector distance ratio. Consequently, $\Delta 2\theta_{hkl}/2\theta_{hkl}$ would be in the range of $\pm 6 \times 10^{-4}$. In the time-of-flight regime of the POLDI diffractometer, the equivalent to $\Delta 2\theta_{hkl}/2\theta_{hkl}$ should be used for comparison: $\Delta \mathrm{TOF}_{hkl}/\mathrm{TOF}_{hkl}$, where TOF_{hkl} is the time-of-flight for a particular *hkl* plane and $\Delta \mathrm{TOF}_{hkl}$ is its shift corresponding to $\Delta 2\theta_{hkl}$ shift. The maximum possible value of the ratio $\Delta \mathrm{TOF}_{hkl}/\mathrm{TOF}_{hkl}$ ($\mathrm{TOF}_{hkl} \sim \sin\theta_{hkl}$ and $\Delta \mathrm{TOF}_{hkl} \sim \cos\theta_{hkl} \cdot \Delta\theta_{hkl}$, thus $\Delta \mathrm{TOF}_{hkl}/\mathrm{TOF}_{hkl} = \operatorname{cotg}\theta_{hkl} \cdot \Delta\theta_{hkl}$) is—for the reflections in the range 75–105° which correspond to the angular extent of PSD—equal to $0.65 \times \Delta 2\theta_{hkl}$ (for $2\theta_{hkl} = 105°$). Therefore, $\Delta \mathrm{TOF}_{hkl}/\mathrm{TOF}_{hkl}$ within the range $-6.5 \div 6.5 \times 10^{-4}$ can be expected. The fit of the peak shifts resulted in $\Delta \mathrm{TOF}_{hkl}/\mathrm{TOF}_{hkl}$ in the range from -3.2 to $+ 3.0 \times 10^{-4}$, which does not exceed the theoretical range and it is thus in very good agreement with the expectation. It means that the explanation of the peak shifts in terms of large-grains holds.

From the preceding out-of-furnace RT measurement, the reference RT values of lattice parameters $a_{\gamma \mathrm{RT}}$ and $a_{\gamma' \mathrm{RT}}$ for IN738LC alloy were known. The evaluation of in-furnace RT measurement thus enables the determination of shifts $\Delta \mathrm{TOF}_{hkl}$ of all visible reflections *hkl* for the sample inside the furnace (i.e., with limited ω-rotation range) with respect to the correct reflection positions TOF_{hkl}.

2.2.3. In-Furnace Measurements at Elevated Temperatures. The measurement up to 1120°C was carried out with the sample B. The diffractograms were taken during holds at constant temperature in the process of rising or decreasing temperature. The measurement time at each temperature was 40 min.

Importantly, the determined set of the shifts $\Delta \mathrm{TOF}_{hkl}$ (see the previous subsection) could be used for high-temperature measurement as the setup of the measurement (slit arrangement, radial collimator, and detector position) as well as the sample position inside the furnace and its rotation range (called altogether geometrical conditions in what follows) did not change during the measurement at elevated temperatures with respect to the geometrical conditions of the in-furnace measurement at RT. During the evaluation of the in-furnace measurements at elevated temperatures, these $\Delta \mathrm{TOF}_{hkl}$ shifts of the peaks can be fixed in the fitting routine and—in turn—the evolution of lattice parameters of γ and γ' can be determined.

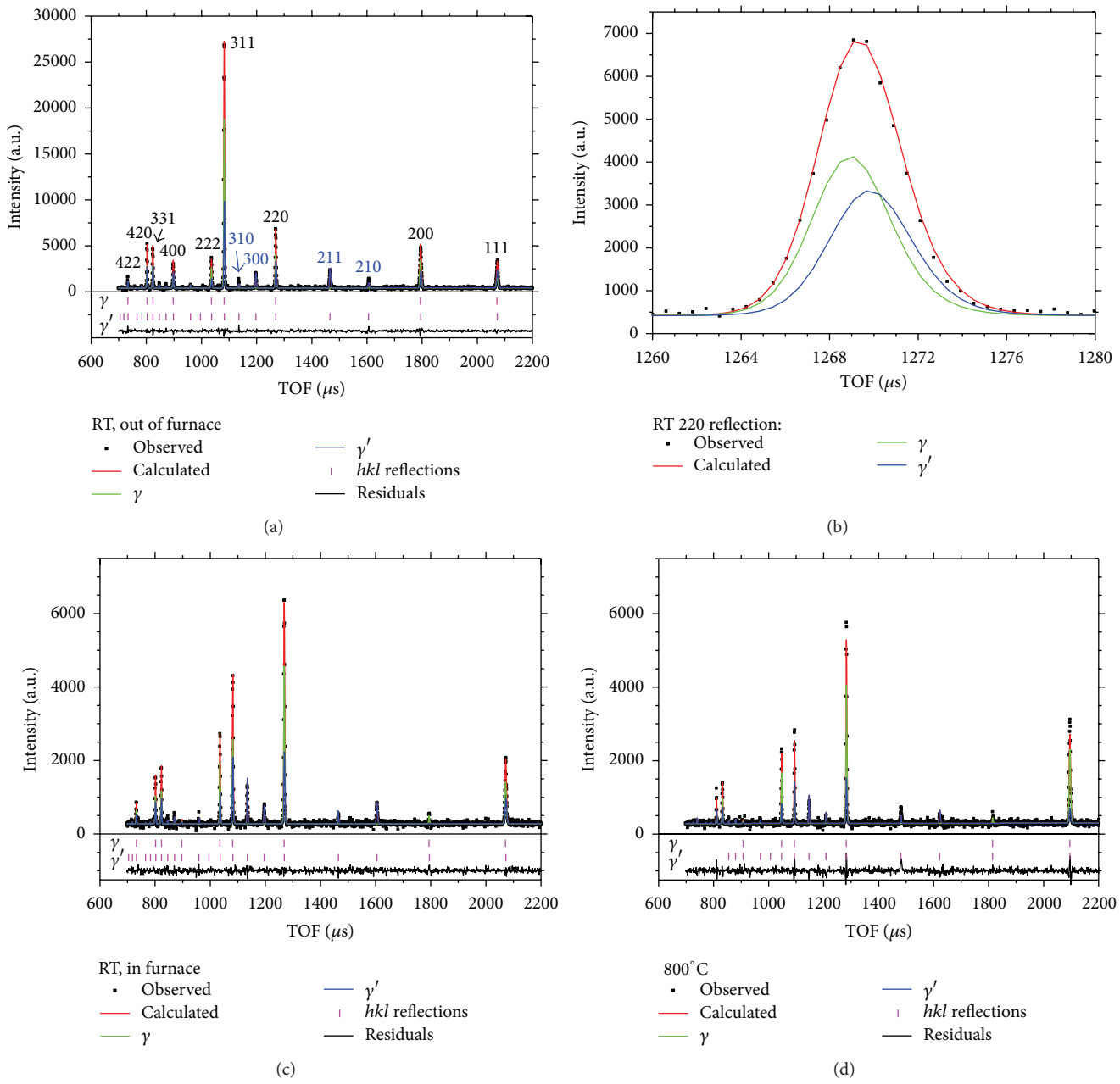

Figure 3: Examples of measured diffractograms of IN738LC. The fit by FullProf, decomposed also to its γ and γ' parts, is plotted, too: (a) out-of-furnace (RT) measurement, (b) detail of 220 reflection for out-of-furnace measurement, (c) in-furnace (RT) measurement, and (d) in-furnace measurement at 800°C. The residuals (observed minus calculated intensity) are shown as well on the bottom part of Figures 3(a), 3(c), and 3(d).

3. Results and Discussion

The examples of diffractograms taken at various conditions for IN738LC samples are plotted in Figure 3. Figures 3(a) and 3(b) correspond to the out-of-furnace measurement, while Figures 3(c) and 3(d) to the in-furnace measurements. As the misfit of the coherent precipitates was very small, the γ and γ' peaks overlap and it was not possible to separate them directly (Figure 3(b) displays a zoomed example of one overlapping peak of γ and γ'). Therefore, the full diffractogram (i.e., not only one γ peak and one γ' peak of the same *hkl* reflection) had to be evaluated. The positional relations between the reflections of γ phase and the relations between the reflections of γ' phase had to be employed in order to obtain the γ and γ' lattice parameters. This was done by using FullProf [17] software.

Preliminary fits showed that it is not possible to perform the standard structure profile refinement. This is—along with the special "frame overlap" setup of the POLDI diffractometer [16]—again due to the fact that the sample has large grains

(i.e., a small number of them in the gauge volume). Some *hkl* reflections are thus strong while others are weak. Therefore, the profile matching (pattern decomposition) option of the FullProf software has to be used. This option enables fitting the scaling factor of each peak individually while keeping fixed the positional relations between all the reflections due to the symmetry of the phase structure.

3.1. Out-of-Furnace Measurement. The RT measurements with permanently ω-rotating (in the 360° range) samples were used for the precise lattice parameter determination of both γ and γ' phase at RT. Due to the symmetry, some reflections (e.g., 310, 300, 211, 210; see Figure 3(a)) were present only for the ordered γ' phase (and not for the disordered γ phase) which helps to determine the lattice parameter of γ' unambiguously. Then, the positions of γ peaks—even though overlapping for all the reflections with the corresponding γ' peaks—could be determined as well.

Generally, γ-phase reflections can be split due to the oriented coherency strains in the γ-channels between γ' precipitates. If the splitting was present in our case, it was so small that it could not be distinguished with the given resolution. As the γ lattice parameter was determined using all the reflections in the diffractogram (i.e. using lattice planes with various orientations relative to the γ-channels), the resulting γ lattice parameter was an orientation average over the whole γ phase volume fraction.

The lattice parameters at RT were found to be $a_{\gamma\mathrm{RT}} = 3.58611(10)$ Å and $a_{\gamma'\mathrm{RT}} = 3.58857(17)$ Å. Average values from two measured samples (A and C) were used. The misfit value at RT was then calculated to be $6.9(6) \times 10^{-4}$, a very low value.

3.2. In-Furnace Measurements. For all measurements with the sample inside the furnace, the shifts of the *hkl* peaks $\Delta\mathrm{TOF}_{hkl}$ (see the procedure for their determination in the "Experimental" section) were fixed. This solves the problem of peak shifts due to large grains for the in-furnace measurements.

Thanks to the reflections which are present only for the ordered γ' phase, the lattice parameter of γ' could be determined unambiguously for all temperatures up to 1000°C. The diffractogram at the highest used temperature 1120°C showed no peaks from γ' as—at this temperature—the precipitates of γ' phase were already dissolved. Thus, the 1120°C measurement provided only the γ phase lattice parameter.

However, there was a complication for the lattice parameter determination of the γ phase at elevated temperatures around 800°C. With increasing temperature, the magnitude of the misfit decreases towards zero which means that—around 800°C—the overlapping peaks of γ and γ' phase could not be unambiguously decomposed (as their centers were positioned at nearly the same place) without an additional constraint concerning the intensity of the peaks.

This constraint can be a fixation of the γ' intensities of those peaks overlapping with γ peaks. Generally, the γ'-peaks intensity is not constant but decreases with increasing temperature due to (i) decrease of γ' volume fraction (gradual precipitate dissolution for temperatures above 800°C) and (ii) increasing thermal diffuse scattering (TDS) which lowers the peak intensities. From the measured data, such decrease of the γ'-peaks intensity with temperature could be estimated. The relative integral-intensity evolution of the reflection 211 (present only for the ordered γ' phase) is plotted in Figure 4. The decrease of the intensity with temperature due to the volume fraction decrease and the TDS effect can be seen. When this dependence was combined with the known RT intensity of the γ'-peaks, the requested fixation of the γ'-peak intensities at elevated temperatures was achieved. It served as the constraint for the evolution of the intensity of all the γ' peaks (also those overlapping with the γ peaks) with temperature during the final fit with FullProf. Although the TDS effect in fact depends on the scattering vector magnitude, the used simple approximation of the intensity decrease (namely, the same dependence for all the peaks) was sufficient for the given purpose and preciseness. As a test that the abovementioned approximation is satisfactory, the diffractograms measured at temperatures 400 and 1000°C—where the misfit is relatively large (with respect to its magnitude at 800°C) and of the opposite sign—were fitted also without the constraint. The resulting misfit was practically the same as with the constraint. It can be thus expected, that the approximation was rather good also for the temperatures in between 400 and 1000°C.

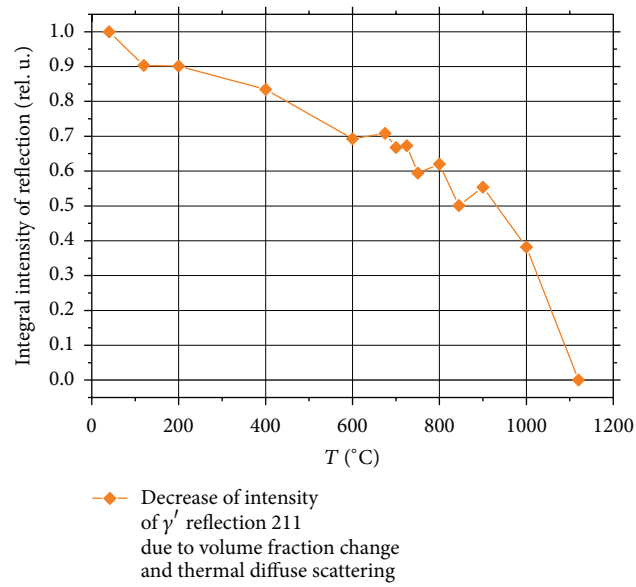

FIGURE 4: The integral intensity of the γ' reflection 211 (after background subtraction) in dependence on temperature.

3.3. Lattice Parameters and Misfit Evolution. Figure 5(a) shows the evolution of the lattice parameters of γ and γ' phases with temperature determined from the in-furnace measured diffractograms of sample B. The results from the measurement of A and C samples, carried out at RT (out of furnace), are added to the graph as well.

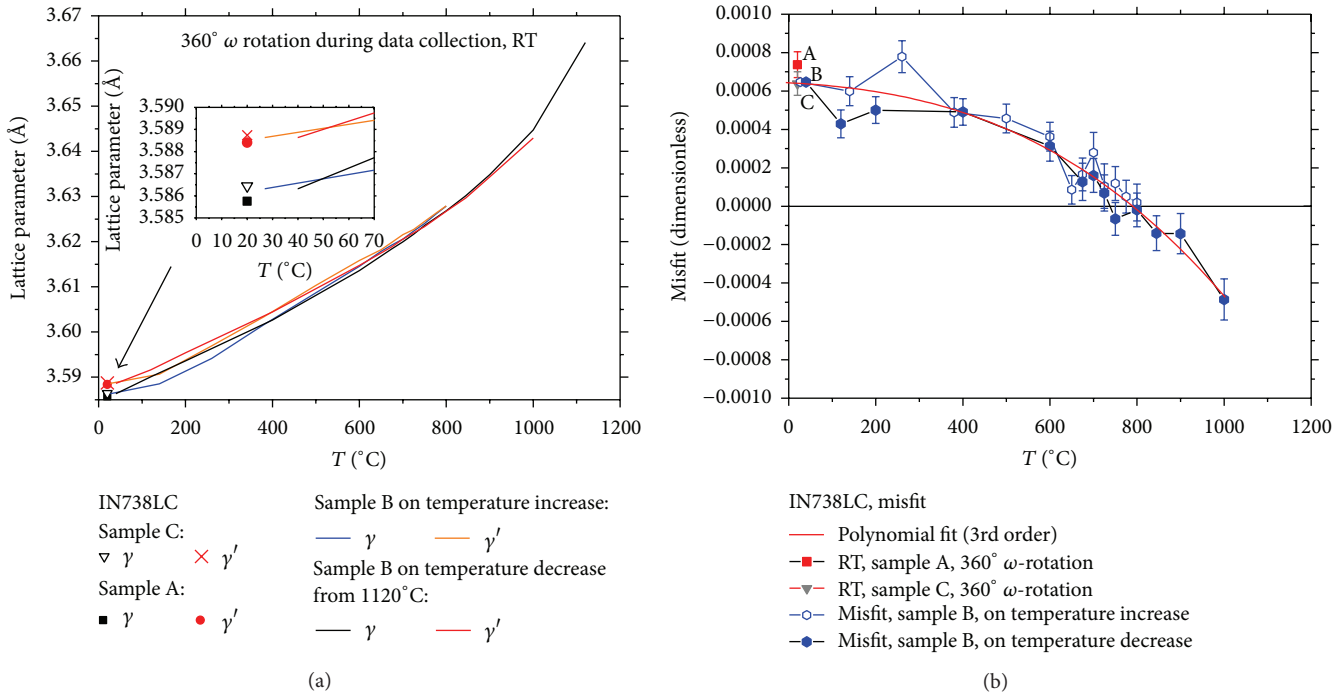

FIGURE 5: (a) Evolution of lattice parameters of γ and γ' in IN738LC superalloy with temperature and (b) temperature dependence on the misfit.

The misfit evolution is shown in Figure 5(b). The temperature dependence of the misfit was interpolated by the 3rd order polynomial. A clear trend of the misfit decrease (from the already low value at RT) with temperature can be seen from the plot. Interestingly, the misfit changes the sign around 800°C and becomes then negative.

4. Conclusions

The misfit in IN738LC alloy was examined at POLDI TOF neutron diffractometer both at room temperature and in situ at elevated temperatures using high-temperature furnace. Due to the large grains in the investigated superalloy, a special setup and evaluation sequence was employed.

Careful out-of-furnace measurement resulted in determination of the lattice parameters of both γ and γ' phases at room temperature (a_γ = 3.58611(10) Å and $a_{\gamma'}$ = 3.58857(17) Å) as well as of the misfit (equal to $6.9(6) \times 10^{-4}$). The room temperature misfit value is rather low.

In situ measurements at elevated temperatures allowed to assessing the evolution of lattice parameters of γ and γ' in IN738LC from RT up to 1120°C. Using these data, the temperature dependence of the misfit was calculated. The misfit decreases with increasing temperature until it reaches zero at around 800°C. Above 800°C, it becomes negative.

The experiment also demonstrates that even a very small misfit (less than 0.1%) and its evolution with temperature can be determined by neutron diffraction though the examined material contains large grains.

Acknowledgments

The support by GACR Project no. P204/11/1453 is gratefully acknowledged. The authors thank SINQ (PSI, Villigen, Switzerland) and NPL (CANAM, NPI Řež, Czech Republic) for providing beamtime and support for ND measurements. Infrastructure projects support (NMI3-II EC Project no. 283883 and CZ MSMT Project no. LM2011019) are gratefully acknowledged as well.

References

[1] E. W. Ross and C. T. Sims, "Nickel-base alloys," in *Superalloys II*, C. T. Sims, N. S. Stoloff, and W. C. Hagel, Eds., chapter 4, pp. 97–134, John Wiley & Sons, New York, NY, USA, 1987.

[2] M. Petrenec, J. Tobiáš, J. Polák, M. Šmíd, A. Chlupová, and R. Petráš, "Analysis of cyclic plasticity of fatigued nickel based superalloys at Elevated Temperautures," in *XVI International Colloquium Mechanical Fatigue of Metals*, J. Polák, T. Kruml, and J. Man, Eds., pp. 245–250, ÚFM AVČR, Brno, Czech Republic, 2012.

[3] R. C. Reed, *The Superalloys: Fundamentals and Applications*, Cambridge University Press, 2006.

[4] H. Harada and H. Murakami, "Design of Ni-base superalloys," in *Computational Materials Design*, T. Saito, Ed., pp. 39–70, Springer, Berlin, Germany, 1999.

[5] G. Bruno and H. C. Pinto, "The kinetics of the γ' phase and its strain in the nickel base superalloy SC16 studied by in-situ neutron and synchrotron radiation diffraction," in *Proceedings of the 10th International Symposium on Superalloys (SUPERALLOYS '04)*, K. A. Green, T. M. Pollock, H. Harada

et al., Eds., pp. 837–846, The Minerals, Metals and Mateials Society, September 2004.

[6] U. Glatzel and A. Müller, "Neutron scattering experiments with a nickel base superalloy part I: material and experiment," *Scripta Metallurgica et Materiala*, vol. 31, no. 3, pp. 285–290, 1994.

[7] D. Siebörger, H. Brehm, F. Wunderlich, D. Möller, and U. Glatzel, "Temperature dependence of lattice parameter, misfit and thermal expansion coefficient of matrix, γ' phase and superalloy," *Zeitschrift fuer Metallkunde*, vol. 92, no. 1, pp. 58–61, 2001.

[8] D. M. Collins, L. Yan, E. A. Marquis et al., "Lattice misfit during ageing of a polycrystalline nickel-base superalloy," *Acta Materialia*, vol. 61, pp. 7791–7804, 2013.

[9] G. Kostorz, Ed., *Treatise on Materials Science and Technology*, Neutron Scattering, Academic Press, New York, NY, USA, 1979.

[10] P. Strunz, M. Petrenec, and U. Gasser, "Precipitate microstructure evolution in low-cycle fatigued Inconel superalloys," in *Proceedings of the 15th International Small-Angle Scattering Conference*, D. McGillivary, J. Trewhella, E. P. Gilbert, and T. L. Hanley, Eds., Australian Nuclear Science and Technology Organisation, Sydney, Australia, November 2012.

[11] P. Strunz, M. Petrenec, U. Gasser, J. Tobiáš, J. Polák, and J. Šaroun, "Precipitate microstructure evolution in exposed IN738LC superalloy," *Journal of Alloys and Compounds*. In press.

[12] M. Šmíd, *Determination of shortcut cyclic stress-strain curves of superalloy INCONEL 738LC at elevated temperatures [Diploma thesis]*, Faculty of Mechanical Engineering, Institute of Material Science and Engineering, Brno, Czech Republic, 2008.

[13] S. Socrate and D. M. Parks, "Numerical determination of the elastic driving force for directional coarsening in Ni-superalloys," *Acta Metallurgica et Materialia*, vol. 41, no. 7, pp. 2185–2209, 1993.

[14] K. Obrtlík, A. Chlupová, M. Petrenec, and J. Polák, "Low cycle fatigue of cast superalloy lnconel 738LC at high temperature," *Key Engineering Materials*, vol. 385-387, pp. 581–584, 2008.

[15] M. Petrenec, M. Šmíd, K. Obrtlík, and J. Polák, "Effect of temperature on the cyclic stress components of Inconel 738LC superalloy," in *Multilevel Approach to Fracture of Materials, Components and Structures: ProceedIngs of the 17th European Conference on Fracture (ECF '08) , Brno, 2–5 September, 2008*, pp. 1358–1365, VUTIUM, Brno, Czech Republic, 2008.

[16] U. Stuhr, H. Spitzer, J. Egger et al., "Time-of-flight diffraction with multiple frame overlap part II: the strain scanner POLDI at PSI," *Nuclear Instruments and Methods in Physics Research A*, vol. 545, no. 1-2, pp. 330–338, 2005.

[17] J. Rodríguez-Carvajal, "Recent advances in magnetic structure determination by neutron powder diffraction," *Physica B*, vol. 192, no. 1-2, pp. 55–69, 1993.